Mon. Not. R. Astron. Soc. **000**, 000–000 (2009) Printed 15 October 2009 (MN LATEX style file v2.2)

The long-term evolution of the accreting millisecond X-ray pulsar Swift J1756.9-2508

Alessandro Patruno[1], Diego Altamirano[1] & Chris Messenger[2]
[1] *Astronomical Institute 'A. Pannekoek', Univeristy of Amsterdam, Science Park 904, Amsterdam, The Netherlands:* a.patruno@uva.nl
[2] *Albert Einstein Institute for Gravitational Research, Callinstraße 38, 30167 Hannover, Germany*

arXiv:0910.2920v1 [astro-ph.HE] 15 Oct 2009

15 October 2009

ABSTRACT
We present a timing analysis of the 2009 outburst of the accreting millisecond X-ray pulsar Swift J1756.9-2508, and a re-analysis of the 2007 outburst. The source shows a short recurrence time of only ~ 2 years between outbursts. Thanks to the approximately 2 year long baseline of data, we can constrain the magnetic field of the neutron star to be 0.4×10^8G $\lesssim B \lesssim 9 \times 10^8$G, which is within the range of typical accreting millisecond pulsars. The 2009 timing analysis allows us to put constraints on the accretion torque: the spin frequency derivative within the outburst has an upper limit of $|\dot{\nu}| \lesssim 3 \times 10^{-13}\,\mathrm{Hz\,s^{-1}}$ at the 95% confidence level. A study of pulse profiles and their evolution during the outburst is analyzed, suggesting a systematic change of shape that depends on the outburst phase.

Key words: X-rays: binaries

1 INTRODUCTION

The accreting millisecond X-ray pulsar (AMXP) Swift J1756.9-2508 (henceforth referred to as J1756) was discovered in 2007 by the Burst Alert Telescope (BAT) aboard the *Swift* satellite (Krimm et al. 2007). Follow up observations were performed with the *RXTE* Proportional Counter Array (PCA) which revealed an X-ray pulsar with a spin frequency of 182 Hz orbiting in 54.7 min around a very low mass companion of minimum mass $0.0067 M_{\odot}$ (Krimm et al. 2007).

The X-ray lightcurve of the 2007 outburst showed a very fast rise of less than 1 day, followed by an exponential decay with an e-folding time of 7.4 ± 0.4 days. An inspection of archival *RXTE* All-Sky Monitor (ASM) data revealed a lack of detections in the previous 10 years of observations, which suggested a long recurrence time for the outbursts. However, due to the low flux of the source and the poor sensitivity of the ASM, the recurrence time was only tentative and a shorter duty cycle was not firmly excluded.

In July 2009 a new outburst was discovered by both *Swift* BAT and *RXTE* PCA observations (Patruno et al. 2009a). Follow-up observations with the *Swift* X-ray telescope (XRT) and *RXTE* PCA were promptly scheduled and monitored the outburst of J1756 until it returned into quiescence.

In this Letter we report a first analysis of the 2009 outburst and a re-analysis of the 2007 data to evaluate the long-term evolution of J1756 on a baseline of approximately 2 years.

2 X-RAY OBSERVATIONS AND DATA REDUCTION

We used all the *RXTE* PCA data (2007 and 2009) and the 2009 *Swift*-XRT observations for J1756 (Table 1). We refer to Jahoda et al. (2006) for PCA characteristics and *RXTE* absolute timing. We used all available Event and GoodXenon data, rebinned to 1/8192 s. For the timing analysis, the photons were extracted from the 2.5-16 keV band to maximize the signal-to-noise ratio (S/N). We barycentered the photons time of arrivals with the FTOOL faxbary by using the source positions as determined from the *Swift*-XRT 2007 observations (Krimm et al. 2007). We folded approximately 500 s long data chunks, keeping only those with S/N> 3.

The fractional sinusoidal amplitude of the i-th pulse profile is calculated as:

$$R_i = \frac{A_i}{N_{ph,i} - B_i} \quad (1)$$

where $N_{ph,i}$ and B_i are the total number of photons and the background counts (calculated with the FTOOL *pcabackest*) in the i-th pulse profile, and A_i is the amplitude (in photon counts) of the observed pulsations. The error on the fractional amplitude R_i is calculated propagating the errors on A_i and $N_{ph,i}$. The error on B_i is negligible with respect to the other errors and will not be considered further. The X-ray lightcurve is constructed by using the counts in PCA Absolute channels 5-37 ($\approx 2.5 - 16$ keV).

During the 2009 outbursts, the *Swift*-XRT observed the faint tail of the outburst with 6 pointed observations (see

Table 1. *RXTE* and *Swift*-XRT observations analyzed for the 2009 outburst

*R*XTE			
Start (MJD)	End (MJD)	Time (ks)	Observation IDs
55026.00	55038.29	183	94065-02-01-* 94065-06-*-*
SWIFT			
55036.71	55047.40	11	00030952014-00030952017 00031455001 00031456001

Table 1) covering a total of $\sim$ 11 ks. All the data were reduced by using the XRT pipeline (v. 0.12.0). Each observation lasted between 1 and 2.2 ks. The data were collected in photon counting (PC) mode and the source and background events were extracted in the energy range 0.5–10 keV, by using circular regions with radii of 20 arcseconds. Given the presence of a very bright source in the proximity of J1756 (GX 5-1) the first four *Swift*-XRT pointings were severely contaminated by the "stray-light" effect (Moretti et al. 2009) which limited the sensitivity of the observations by increasing the background contamination.

For the spectral analysis we extracted PCA and HEXTE spectra from the standard modes following the procedures suggested by the RXTE team[1], using the latest available version of the analysis tools by September 1st, 2009. For the PCA we only used data of PCU 2, which was active in all observations. For HEXTE we only used data from Cluster B. No energy channels were binned in any case. No systematic errors were added to HEXTE data, while we used the standard 0.5% for the PCA data. We fitted simultaneously the PCA and HEXTE data in the 3–25 and 25–150 keV range, respectively. A single absorbed blackbody or a single power law component did not fit well the data, so we used a standard absorbed *wabs* (Morrison & McCammon 1983) three-components model (disc-blackbody, a power law and a Gauss line if necessary). To fit the data we used Xspec v12.5.0 (Arnaud 1996). We tried also to fit *compTT* (Titarchuk 1994) and *compPS* (Poutanen & Svensson 1996) spectral models. In all cases we obtained a satisfactory fit with reduced $\chi^2 \sim 0.8 - 1.01$ for 82 or 83 degrees of freedom (depending on the model used).

3 RESULTS

3.1 X-ray lightcurve

We extracted the 2.5-16 keV X-ray flux from the *RXTE*-PCA and *Swift*-XRT observations. The lightcurve is shown in Figure 1. The rising portion of the lightcurve is missing because the *RXTE* monitoring started approximately five days after the beginning of the outburst(Patruno et al. 2009a). The lightcurve shows a slow decay for ~ 5 days before entering a fast decay phase (marked with the vertical dashed line in the figure) that brings the luminosity down to the detection level of *RXTE* on a timescale of ~ 2 days. The slow-decay portion of the lightcurve is well fitted by an exponential decay law with an e-folding time of 10.2 ± 0.1 days. The fast-decay has an e-folding time of 2.7 ± 0.1 days. Both these two values are longer than the timescales reported by Krimm et al. (2007) for the 2007 outburst (7.6 ± 0.4 and 0.6 ± 0.3 days for slow and fast decay respectively; see Figure 1). After only 3 days from the last *RXTE*-PCA detection, the *Swift*-XRT was unable to detect the source. The upper limit on the flux level at this time was 100 times smaller than that estimated from the last *RXTE*-PCA observation, and indicates that the source was probably returned into quiescence.

3.2 Color-Color Diagram

We use the 16 s time resolution Standard 2 mode data to calculate X-ray colours. Hard and soft colours are defined, respectively, as the 9.7-16.0 keV/6.0-9.7 keV and the 3.5-6.0 keV/2.0-3.5 keV count rate ratios. The energy-channel conversion is done by using the pca_e2c_e05v02 table provided by the RXTE team. The background was subtracted and dead-time corrections were made. In order to correct for the gain changes and the differences in effective area between the PCUs themselves, we normalized our colours by the corresponding Crab Nebula color values (see Kuulkers et al. 1994; van Straaten et al. 2003) that are closest in time but in the same RXTE gain epoch, that is, with the same high voltage setting of the PCUs (Jahoda et al. 2006). During the 2009 observations, the source was always in the so-called island/extreme island state, which is typical of persistent AMXPs. The source was also in the island/extreme island state (not shown) during the 2007 outburst, as reported by Linares et al. (2008), that identified J1756 as a typical atoll source. The colours of the source are consistent among the two outbursts.

3.3 Coherent timing analysis of the 2009 outburst

We fitted each pulse profile with a constant plus two sinusoids: one at the nominal pulse frequency and the other at twice the pulse frequency, representing the fundamental and the first overtone, respectively. We then selected only pulses with a ratio between the amplitude and its statistical error larger than 3. Several significant first overtones were found. We therefore analyzed separately the fundamental and the first overtone, as described in Patruno et al. (2009b).

We fitted the time of arrivals of each pulse profile with a circular keplerian model plus a linear term representing the neutron star spin frequency. We used the pulsar timing program TEMPO2, which minimizes the timing residuals between the predicted and the observed arrival times of the pulsations (Hobbs et al. 2006). After obtaining a converged solution we re-iterated for a few times the whole procedure: using the improved solution we re-folded our pulse profiles and re-fitted our time of arrivals until convergence. The fit is statistically satisfactory for the fundamental (reduced $\chi^2 = 1.0$ for 251 degrees of freedom) while it is not acceptable for the first overtone (reduced $\chi^2 = 2.8$ for 73 dof). The reason why the first overtone shows a bad fit relies on the presence of X-ray timing noise in the pulse phases. The timing noise operates on rather short timescales, producing jumps in the

[1] http://heasarc.gsfc.nasa.gov/docs/xte/xtegof.html

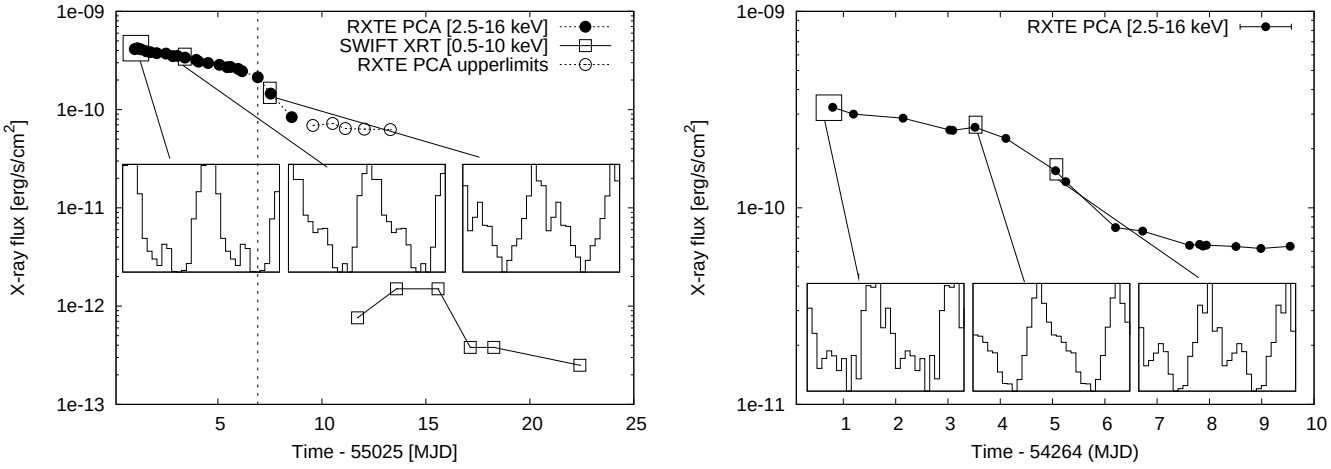

Figure 1. X-ray lightcurve and pulse profile evolution of 2009 (left panel) and 2007 (right panel) outbursts. **Left Panel:** RXTE-PCA [2.5-16 keV] and Swift XRT [0.5-10 keV] lightcurve of the 2009 outburst of J1756. The open circles and the open squares refer to 95% confidence level upper limits. The vertical dashed line identifies the beginning of the fast decay. The strong contamination of the nearby source GX 5-1 affected both the flux determinations of RXTE-PCA and Swift-XRT (see text for details). The three panels in the center show the pulse profile evolution (two cycles are plotted for clarity) obtained when folding a small chunk of lightcurve. **Right Panel:** RXTE-PCA [2.5-16 keV] lightcurve of the 2007 outburst, shown for comparison

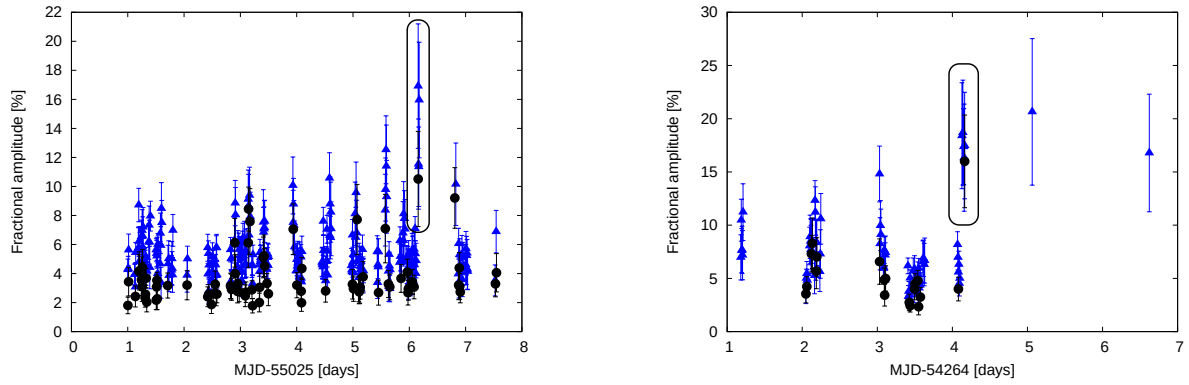

Figure 2. Fractional amplitude vs. time for the 2009 (left panel) and 2007 (right panel) outburst of J1756. The fundamental is indicated with blue triangles and the first overtone with black filled circles. The fractional amplitude varies between approximately 2 and 20% during the two outbursts. The two circled groups of points, that show a substantial increase in pulsed fraction, refer to the beginning of the fast decay.

timing residuals of up to 0.12 cycles on a timescale of a few hours. This is not observed in the fundamental, where the phase behaviour is smooth throughout the outburst. To partially take into account the presence of timing noise in the first overtone, we increased the statistical errors on the pulse phases of the first overtone by a factor 1.7. The orbital and spin parameters of the 2009 outburst, along with upper limits on the spin frequency derivative and the eccentricity are reported in Table 2.

We repeated the coherent timing analysis of the *RXTE*-PCA observations of the 2007 outburst of J1756 (see Krimm et al. 2007 for a similar timing study of the 2007 outburst). Also in this outburst several significant first overtones are detected in the pulse profiles. The timing solution for the 2007 outburst is reported in Table 3. In this case both the fundamental and the first overtone show a low, but significant, amount of X-ray timing noise in the pulse phases. We rescaled the pulse phase statistical errors by a factor 1.2 and 1.4 respectively, to partially take into account this effect when estimating the timing parameter uncertainties.

The pulse fractional amplitudes, as defined in Eq. 1, are reported in Figure 2 (note that this is the *sinusoidal fractional amplitude*, as defined in Eq. 1, which is a factor $\sqrt{2}$ larger than the fractional rms amplitude). The pulsed fraction of the fundamental fluctuates between 2 and $\sim$ 20% during both outbursts, while the first overtone reaches a maximum amplitude of 10-15% and a minimum value of 2%. The fractional amplitudes increase substantially in correspondence with the beginning of the *fast decay* (see circled points in Fig. 2 and vertical dashed line in Fig. 1). Interestingly, after the beginning of the 2009 fast decay, the fractional amplitudes return back to values comparable to the rest of the outburst.

We also studied the energy dependence of the pulsed

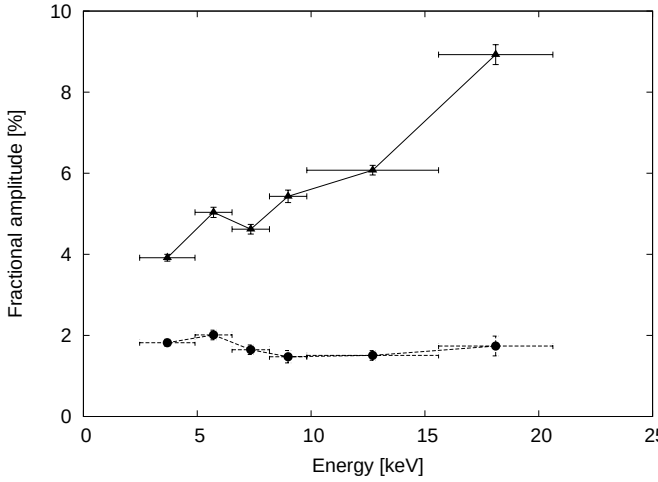

Figure 3. Fractional amplitude vs. energy for the 2009 outburst of J1756. The fundamental is indicated with black triangles and the first overtone with black filled circles. The fractional amplitude of the fundamental increases with energy (apart from a small decrease around $\sim 6-7$keV).

‘

fractions for the 2009 outburst (see Figure 3). The amplitude of the fundamental increases with energy, with a slope of $0.28\pm0.02\%$ keV^{-1}, although it is evident a slight decrease in amplitude in the 6-7 keV energy bin. The first overtone instead remains approximately constant with a slight decrease of amplitude above 6 keV.

3.4 Emission lines in the X-ray spectrum

We searched for the presence of emission lines in the broad-band spectrum of the longest RXTE observation. In this way our statistics are the best and at the same time we are sure that the spectrum has not changed significantly in time.

A line is clearly detected in the 6-7 keV band, in several occasions. For example, in Figure 4 we show the ratio of the data to the continuum model. In this particular case, the flux of the line is $(8\pm2)\times10^{-4}$ photons cm^{-2} s^{-1}. We also performed a similar analysis on data from the 2007 outburst; we found several cases with significant emission lines in the same energy range as in 2009. Although we cannot confirm the nature of the line in the data, the detection could be suggestive of the presence of an Iron line. The low energy resolution of our RXTE data does not allow us to constrain with high accuracy the energy of the line, the emissivity index, the inner radii of the disc and/or the inclination of the system. It is also hard to constrain the presence of a Compton reflection bump in the X-ray spectrum because of the poor statistics given by the very low number of counts at high energies. XMM-Newton, Chandra or Suzaku observations are needed to verify the nature of the line.

4 DISCUSSION

4.1 Pulse profiles

The pulse profile shape of J1756 shows a substantial variability during the two outbursts. Pulse shape variability is related with the variability of pulse phases and the variation of pulse amplitudes with time. The pulse profiles appear to have a similar evolution in the two outbursts, with similar profile shapes for similar outburst phases (see Fig. 1). In particular, the profiles start with an almost sinusoidal shape that evolves in time and turns into a skewed profile during the slow decay and becomes double peaked during the fast decay stage. Unfortunately, due to low counting statistics, it was not possible to further follow the evolution of the pulse profiles as the source returns to quiescence. However, it appears intriguing the similarity of this behaviour with that of SAX J1808.4-3658 (Hartman et al. 2008, Hartman et al. 2009), where the pulse profiles exhibit a similar evolution of shapes between outbursts. The presence of a stronger secondary bump toward the end of the outburst is also interesting in light of the antipodal spot obscuration model recently proposed by Ibragimov & Poutanen (2009). The authors propose a receding inner accretion disc as a possible cause of obscuration of the antipodal spot, that slowly re-emerges toward the end of the outburst, when the disc is emptying. This moves the antipodal hot spot into the line of sight of the observer and increases the relative strength of the first overtone over the fundamental, thus producing a stronger secondary bump in the pulse profile.

4.1.1 Timing noise

The study of the 2009 pulse phases reveals a lack of timing noise in the pulse phases of the fundamental, and a short-timescale timing noise on the first overtone. This appears opposite to previous studies in which the first overtone has been considered somehow more stable than the fundamental.

We repeated the analysis of the 2007 outburst to check the long-term spin and orbital evolution of J1756. Our orbital solution is consistent with that reported in Krimm et al. (2007) (see also the erratum Krimm et al. 2009 for a correction on the value of T_{asc}). We found also an offset of 0.32μHz from the spin frequency reported in Krimm et al. (2007). The reason of this discrepancy is more subtle and probably has to be identified in the difference between the timing techniques adopted in this paper and in Krimm et al. (2007). Indeed, Krimm et al. (2007) did not perform an analysis of the fundamental and first overtone separately. As shown by Hartman et al. (2008) and Patruno et al. (2009b), significant deviations from the true timing solution arise when performing a coherent study in presence of pulse profile variability.

The new improved set of ephemeris is not only important for the interpretation of the X-ray data, but is crucial for understanding the long term evolution of the neutron star spin and for any radio-search for pulsations in this AMXP.

Table 2. Timing solution for Swift J1756–2508 (**2009 outburst**)

Parameter	Fundamental	First overtone
Spin frequency ν (Hz)	182.06580391(2) Hz	182.06580393(5)
Spin frequency derivative $\dot{\nu}$ (Hz/s)	$< 3 \times 10^{-13}$ (95% c.l.)	$< 1.2 \times 10^{-12}$ (95% c.l.)
Orbital period (s)	3282.32(3)	3282.38(6)
Projected semimajor axis (lt-ms)	5.98(2)	5.96(3)
Time of passage to the ascending node (MJD)	55026.03431(3)	55026.03425(6)
Eccentricity	< 0.01 (95% c.l.)	< 0.01 (95% c.l.)
χ^2/dof	250.9/251	71.0/73[a]

[a] The value of χ^2 refers to the fit where the pulse phase uncertainties have been rescaled by a factor 1.7

Table 3. Timing solution for Swift J1756–2508 (**2007 outburst**)

Parameter	Fundamental	First overtone
Spin frequency ν (Hz)	182.06580393(7) Hz	182.06580378(24)
Spin frequency derivative $\dot{\nu}$ (Hz/s)	$< 3 \times 10^{-12}$ (95% c.l.)	$< 1.6 \times 10^{-11}$ (95% c.l.)
Orbital period (s)	3282.41(15)	3282.27(26)
Projected semimajor axis (lt-ms)	5.95(4)	6.04(6)
Time of passage to the ascending node (MJD)	54265.28087(10)	54265.28078(14)
Eccentricity	< 0.03 (95% c.l.)	< 0.03 (95% c.l.)
χ^2/dof	59.94/63[a]	13.12/14[b]

[a] The value of χ^2 refers to the fit where the pulse phase uncertainties have been rescaled by a factor 1.2. [b] The value of χ^2 refers to the fit where the pulse phase uncertainties have been rescaled by a factor 1.4.

4.1.2 Pulse amplitudes

The pulse profiles of J1756 have two remarkable features: a steep increase of fractional amplitudes with energy and a sudden increase of amplitude in correspondence with the beginning of the fast decay.

The energy dependence of the profiles is not new among AMXPs, as it has been already observed and discussed in three sources: IGR J00291+5934 (Falanga et al. 2005), Aql X-1 (Casella et al. 2008) and SAX J1748.9-2021 (Patruno et al. 2009c). A possible reason for this is given by photoelectric absorption around the rotating hot spots. A very similar slope of the linear relation governing the amplitude energy dependence was reported for the intermittent source SAX J1748.9-2021 (Patruno et al. 2009c). However, SAX J1748 and Aql X-1 (both intermittent pulsars) were observed to pulsate in the soft state (Casella et al. 2008, Altamirano et al. 2008), while J1756 is in the hard state (as IGR J00291), which is a more common feature among AMXPs. This suggests that the observed increase of pulsed amplitudes with energy is not a specific feature of intermittent sources nor of soft or hard states.

More difficult to explain is the sudden increase of fractional amplitude of both harmonics with the beginning of the fast decay. Alternate variations of pulse amplitudes after the beginning of the fast decay were already observed in the pulsed fractions of SAX J1808.4-3658 (see Fig. 1 in Hartman et al. 2008). These increase might be connected with some fundamental readjustment of the accretion disc that corresponds to the onset of the fast decay (see Lasota 2001 for a review of the different outburst stages).

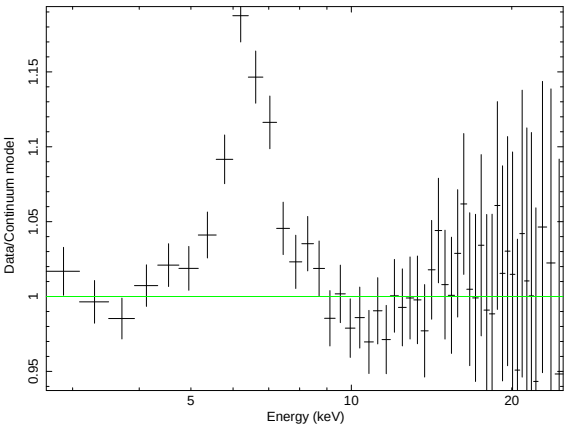

Figure 4. Ratio of the data to the continuum model. The flux of the line is $(8 \pm 2) \times 10^{-4}$ photons cm^{-2} s^{-1}. These dataset correspond to ObsID:94065-06-02-04.

4.2 Torques during outbursts

Upper limits on any spin frequency derivative (both spin up and spin down) can be made using the coherent timing analysis of the 2009 outburst: $|\dot{\nu}| \lesssim 3 \times 10^{-13}\,\mathrm{Hz\,s^{-1}}$ at the 95% confidence level. If standard accretion torque theory is correct, the magnetospheric radius (r_m) should decrease with the increase of the mass accretion rate $\dot{M}$, following a power-law $r_m \propto \dot{M}^{-\alpha}$ when $r_m < r_{co}$, with $\alpha = 2/7$ in the simplest case. The term r_{co} is the the co-rotation radius. Assuming a source distance of 8 kpc (Krimm et al. 2007), the expected mass transfer rate at the peak of the outburst is $\dot{M} \approx 8 \times 10^{-10} M_\odot\,\mathrm{yr^{-1}}$. The expected spin frequency derivative is:

$$\dot{\nu} = \frac{\dot{M}\sqrt{GMr_m}}{2\pi I} \simeq 1.6 \times 10^{-13}\,\mathrm{Hz\,s^{-1}} \times \left(\frac{\dot{M}}{10^{-10} M_\odot\,\mathrm{yr^{-1}}}\right)\left(\frac{\nu}{\mathrm{Hz}}\right)^{-1/3}\left(\frac{r_m}{r_{co}}\right)^{1/2} \quad (2)$$

Therefore the expected maximum spin frequency derivative for J1756 has to be of the order of $2 \times 10^{-13}\,\mathrm{Hz\,s^{-1}}$, which is within our measured upper limits.

4.3 Torques during quiescence

By using the spin frequencies of 2007 and 2009 outbursts we can also put some upper limits on the presence of a spin frequency derivative during quiescence. The difference in frequencies between the 2007 and 2009 is 0.02μHz, which is within the uncertainties of the frequency determination. By propagating the uncertainties on the 2007 and 2009 spin frequencies, we can obtain an upper limit for any change in spin frequency during quiescence: $|\Delta\nu| \lesssim 0.12\mu$Hz (95% confidence level) and therefore $|\dot{\nu}| \lesssim 2 \times 10^{-15}\,\mathrm{Hz\,s^{-1}}$ (95% c.l.). This value is not particularly constraining, and is a factor 4 larger than the value measured by Hartman et al. (2008, 2009) for the pulsar SAX J1808.4-3658.

By using the relativistic force-free MHD models of pulsar magnetospheres described by Spitkovsky (2006), we expect a magneto-dipole torque:

$$N_{\mathrm{dipole}} = -\mu^2 (2\pi\nu/c)^3 (1+\sin^2\alpha) \quad (3)$$

where μ is the magnetic dipole moment and α is the angle between the magnetic and rotational poles. This provides an upper limit on the magnetic dipole moment and therefore on the pulsar magnetic field:

$$\begin{aligned}\mu \;<\; & 4.5\times10^{26}\left(1+\sin^2\alpha\right)^{-1/2} \\ & \times\left(\frac{I}{10^{45}\ \mathrm{g\ cm^2}}\right)^{1/2}\left(\frac{\nu}{182\ \mathrm{Hz}}\right)^{-3/2} \\ & \times\left(\frac{-\dot{\nu}}{1.8\times10^{-15}\ \mathrm{Hz\ s^{-1}}}\right)^{1/2}\ \mathrm{G\ cm^3}\,. \end{aligned} \quad (4)$$

By assuming $\alpha = 0$, we obtain an upper limit for the neutron star magnetic field of $B < 9 \times 10^8$G. If J1756 is located close to the Galactic Center at a distance of 8 kpc, a lower limit for the magnetic field can be calculated by using the same argument as in Psaltis & Chakrabarty (1999), which assumes that the B field is strong enough to channel the accreting gas at the maximum mass accretion rate. By using the value $\dot{M} \approx 8\times10^{-10}\mathrm{M_\odot\,yr^{-1}}$ we obtain a magnetic field range of:

$$0.4 \times 10^8 G \lesssim B \lesssim 9 \times 10^8 G \quad (5)$$

These values are similar to those obtained for other AMXPs and confirm the rather narrow range of neutron star magnetic fields in accreting systems.

4.4 Emission lines and X-ray spectrum

The presence of an emission line in the 6-7 keV range suggest the intriguing possibility of an Iron line in the broadband spectrum of J1756. A broad relativistic Iron line has been detected only in one AMXP until now (Papitto et al. 2009,Cackett et al. 2009), and its detection in J1756 can help to strongly constrain the inner accretion disc radius and the neutron star magnetic field strength. However, care has to be used when claiming the detection of Iron lines in X-ray binaries, since we do not detect a Compton reflection bump in the X-ray spectrum and we do not have a sufficient spectral resolution to verify whether the line is composed by a superposition of narrow lines or whether it is a single genuinely relativistically broadened line. The reason why we do not detect a Compton bump in our data can be due to a lack of statistics at high energies, and a deeper observation is required to verify the Iron line hypothesis.

5 CONCLUSIONS

Swift J1756.9-2508 has shown a short recurrence time of only two years and it is the optimal candidate to study the long-term evolution of neutron star spin and orbital parameters.

The pulse profiles evolve in time with strong similarities between the two outbursts and show a steep increase of pulsed fraction with energy. With the increasing number of AMXPs exhibiting an hard energy dependence of pulse amplitudes, it becomes more likely to discover new AMXPs among the large family of the non pulsating low mass X-ray binaries. Indeed, all the 12 AMXPs discovered until now have been observed with X-ray telescopes which are sensitive to energies below 20 keV, or that are not designed to perform efficient coherent X-ray timing observations. With the forthcoming X-ray telescopes like ASTROSAT, which will have a very high effective area up to $\sim$ 80 keV, the detection of AMXPs with rising pulsed fractions at hard energies could be much easier and efficient.

The pulse phases show a low, but significant, timing noise content and special techniques have to be applied to determine the neutron star spin evolution. Thanks to the measurement of timing parameters in two outbursts, we can now set the first constraints on the neutron star magnetic field ($0.4 \times 10^8 G \lesssim B \lesssim 9 \times 10^8$G) that makes this neutron star a typical member of the AMXP family.

ACKNOWLEDGMENTS

We would like to thank the *RXTE* and the *Swift* team for promptly scheduling the observations of the 2009 outburst. We would like to thank also Tod Strohmayer and Craig Markwardt for useful support during the observations and Rudy Wijnands and Anna Watts for useful discussions.

REFERENCES

Altamirano, D., Casella, P., Patruno, A., Wijnands, R., & van der Klis, M. 2008, ApJL, 674, L45

Arnaud, K. A. 1996, Astronomical Data Analysis Software and Systems V, 101, 17

Cackett, E. M., Altamirano, D., Patruno, A., Miller, J. M., Reynolds, M., Linares, M., & Wijnands, R. 2009, ApJL, 694, L21

Casella, P., Altamirano, D., Patruno, A., Wijnands, R., & van der Klis, M. 2008, ApJL, 674, L41

Falanga, M., et al. 2005, A&A, 444, 15

Hartman, J. M., Patruno, A., Chakrabarty, D., Kaplan, D.L., Markwardt, C.B., Morgan, E.H., Ray, P.S., van der Klis, M., Wijnands, R., 2008, ApJ, 675, 1468

Hartman, J. M., Patruno, A., Chakrabarty, D., Markwardt, C. B., Morgan, E. H., van der Klis, M., & Wijnands, R. 2009, ApJ, 702, 1673

Hobbs, G. B., Edwards, R. T., & Manchester, R. N. 2006, MNRAS, 369, 655
Ibragimov, A., & Poutanen, J. 2009, MNRAS, 1322
Jahoda, K., Markwardt, C. B., Radeva, Y., Rots, A. H., Stark, M. J., Swank, J. H., Strohmayer, T. E., & Zhang, W. 2006, ApJS, 163, 401
Krimm, H. A., et al. 2007, The Astronomer's Telegram, 1105, 1
Krimm, H. A., et al. 2007, ApJL, 668, L147
Krimm, H. A., et al. 2009, ApJL, 703, L183
Kuulkers, E., van der Klis, M., Oosterbroek, T., Asai, K., Dotani, T., van Paradijs, J., & Lewin, W. H. G. 1994, A&A, 289, 795
Lasota, J.-P. 2001, New Astronomy Review, 45, 449
Linares, M., Wijnands, R., van der Klis, M., Krimm, H., Markwardt, C. B., & Chakrabarty, D. 2008, ApJ, 677, 515
Moretti, A., et al. 2009, A&A, 493, 501
Morrison, R., & McCammon, D. 1983, ApJ, 270, 119
Papitto, A., Di Salvo, T., D'Aì, A., Iaria, R., Burderi, L., Riggio, A., Menna, M. T., & Robba, N. R. 2009, A&A, 493, L39
Patruno, A., Markwardt, C. B., Strohmayer, T. E., Swank, J. H., Smith, S. E., & Pereira, D. 2009a, The Astronomer's Telegram, 2130, 1
Patruno, A., Hartman, J. M., Wijnands, R., Chakrabarty, D., & van der Klis, M. 2009b, arXiv:0902.4323
Patruno, A., Altamirano, D., Hessels, J. W. T., Casella, P., Wijnands, R., & van der Klis, M. 2009c, ApJ, 690, 1856
Poutanen, J., & Svensson, R. 1996, ApJ, 470, 249
Psaltis, D., & Chakrabarty, D. 1999, ApJ, 521, 332
Spitkovsky, A. 2006, ApJL, 648, L51
Titarchuk, L. 1994, ApJ, 434, 570
van Straaten, S., van der Klis, M., & Méndez, M. 2003, ApJ, 596, 1155